Research Article GU J Sci 38(2): 780-790 (2025) DOI: 10.35378/gujs.1505025

Gazi University

Journal of Science

http://dergipark.gov.tr/gujs

Quad Element Metamaterial based Antenna for C and X band Application with Improved Diversity Characteristics

Sumit Kumar GUPTA*, Aditi SHARMA, Soma DAS

Department of ECE, SoS of Engineering a& technology, Guru Ghasidas Vishwavidyalaya Bilaspur India

Highlights

- The metamaterial superstrate is placed at 1.5 mm above the MIMO results in less design volume.
- UWB characteristics with isolation below -30dB in the entire UWB band
- The design exhibits ECC, DG, CCL, MEG well below acceptable limits showing its diversity behavior.

Article Info

Received: 26 Jun 2024
Accepted: 25 Dec 2024

Keywords

Fractal
Isolation
MIMO
Gain
Diversity

Abstract

In this paper a metamaterial loaded UWB MIMO operating in C and X band is presented. The proposed design uses hexagonal fractal structure with partial ground plane to achieve UWB characteristics. The design is utilized for four element MIMO to offer better diversity performance with relevant compactness. The isolation between orthogonally placed MIMO elements is achieved below -15dB in entire resonance band from 6 GHz to 12 GHz with inter-element separation of 0.33λg giving the overall dimension of 93mm x 93mm x 1.6mm. The isolation is further enhanced by using a single negative (SNG) metamaterial with MIMO. The obtained results were verified by fabricating the proposed design in low-cost FR-4 showing the resonance from 6-12 GHz with good impedance matching and isolation below -30 dB in entire resonating band. The uniqueness of the proposed design is much less volume despite the metamaterial superstrate placed 1.5 mm above the MIMO. The 2D radiation pattern for E field and H field co and cross polarization shows more co-polarization and less cross polarization with almost omnidirectional radiation pattern.

1. INTRODUCTION

Due to technical advancement, the demand for large bandwidth, good channel capacity with low losses and appreciably diverse MIMO antenna with relative compactness is increasing day by day. Number of works has been reported in the past which proves MIMO antenna leads to the competitions in terms of miniaturization, large bandwidth, and diverse behavior with required isolation between elements placed in close proximity to achieve compactness [1]. In the past to achieve required features Several works have been carried out which includes use of fractal antenna [2], complementary split ring resonator [3], FSS structure [4], SRR Structure [5], electromagnetic band structure (EBG) [6], defected ground structures [7], different types of slot in the patch and the ground [8], Orthogonal placement of MIMO [9], use of circular polarization and CSRR structure [10], to name a few. Further the required improvement in isolation and diversity characteristics needs investigations of more prominent methods like use of metamaterials in the related literatures. In the recent past metamaterial-based structures are placed either between the radiating elements or in the ground, or as parasitic or as superstrate to achieve required improvement in gain, isolation, and diversity characteristics [11-17]. A Single Negative (SNG) metamaterial based FSS placed in back side of antenna [11], FSS with negative permeability and permittivity between the antenna elements acting as band-stop filter [12]. In [13], a metamaterial superstrate results in isolation below -15 dB and gain enhanced by 1.2dB. In another work LC shaped metamaterial exhibiting negative refractive index and negative permittivity-based resonator is used for bandwidth enhancement [14]. A Hexagonal shaped meta-surface [15], high refractive index metamaterial [16], stacked multilayer Metasurface were applied as superstrate [17] for improvement of gain. Metamaterial structures also help in achieving miniaturization along with required isolation [18-23]. The attempt was made in [24] to address to improve isolation by

*Corresponding author, e-mail: sgupta@ggu.ac.in

application of resistance loaded stub and results in better than 15 dB isolation. In [25-27], metamaterial-based structures are again utilized for improvement of gain and isolation but at the same time results in large design area and volume due to placement of metamaterial. Based on the above review, it can be estimated that the metamaterials can be utilized as superstrate or in between the radiating element or in the ground plane to change the flow of surface waves in such a direction that would result in improvement of gain, isolation, and other diversity parameters.

In the present work, we have used SNG metamaterial of the same dimension as of antenna, loaded above the radiating element at very short distance of 1.5mm as compared to earlier designs discussed in introduction section, which results in relative compactness in volume, improvement in isolation by about 15dB along with gain improvement in entire operating band. The diversity parameters like ECC, DG, CCL, MEG, are calculated for the design which clearly proves the design to be well versed with the competitions in C and X band applications.

2. DESIGN AND GEOMETRY OF FOUR ELEMENT MIMO WITHOUT AND WITH METAMATERIAL SUPERSTRATE

2.1. Design of Four Element MIMO without Metamaterial Superstrate

The four-element orthogonally placed MIMO antenna is designed in low-cost FR-4 material with copper patch due to advantage of high gain and directivity over other metals. Design evolution started with a single-element UWB antenna, as shown in Figure 1(a). Fractal ring added either result in addition of resonance in lower frequency region or in result in better impedance matching which finally helps in getting multiband response with better matching. Ground plane modification helps in bandwidth improvement by merging multiband resonance into UWB response in the C and X bands as shown in Figure 1 (b). Further to enhance diversity performance, data rate and reliability, the design is extended to MIMO antenna where the antenna elements are placed side by side at very short distance of 6 mm to achieve required compactness. The nearby placement of radiators results in degraded isolation of 6dB between the elements as shown in Figure 1(c). For isolation enhancement, orthogonal placement of radiator is applied to four element MIMO resulting in isolation enhanced to -13dB in entire C and X band. The front and back view of four element orthogonally placed antenna along with corresponding S parameter are shown in Figure 1(d), 1(e) and 1(f) respectively [24].

The design dimensions of the MPA are

Warray=93mm, Larray=93, x1= 29.6, x2= 60.5, L1=11.41, a=18, b=15, c=13, d=10, e=8.5, f=7, g=5.9, h=4.9 i=3, j=2.84, k=1.5, l=1, x3=44, x4=11, x6=1, L2=33 (all design dimensions are in mm).

The orthogonal placement of radiating element results in reduced mutual coupling between elements 1-2 (Minimum S21 is -22 dB) and 1-4 (Minimum S41 is -22 dB) but the mutual coupling is around -13dB between 1-3 (S31=-13 dB) as shown in Figure 1 (f). To further address isolation, metamaterial structures are studied and single negative (SNG) metamaterial superstrate array is designed which gives either ENG or MNG in the entire C and X band. The designed SNG metamaterial is placed above four elements orthogonally placed microstrip patch antenna.

2.2. Geometry of the SNG Metamaterial Superstrate

The SNG metamaterial evolution stages and its corresponding extracted parameters are shown in Figure 2 (a). In the design, the Outer Copper Frame (w1, l1, and l7) contributes to the overall inductance and capacitance of the unit cell and sets fundamental resonance frequency and creates the baseline for negative permittivity or permeability.

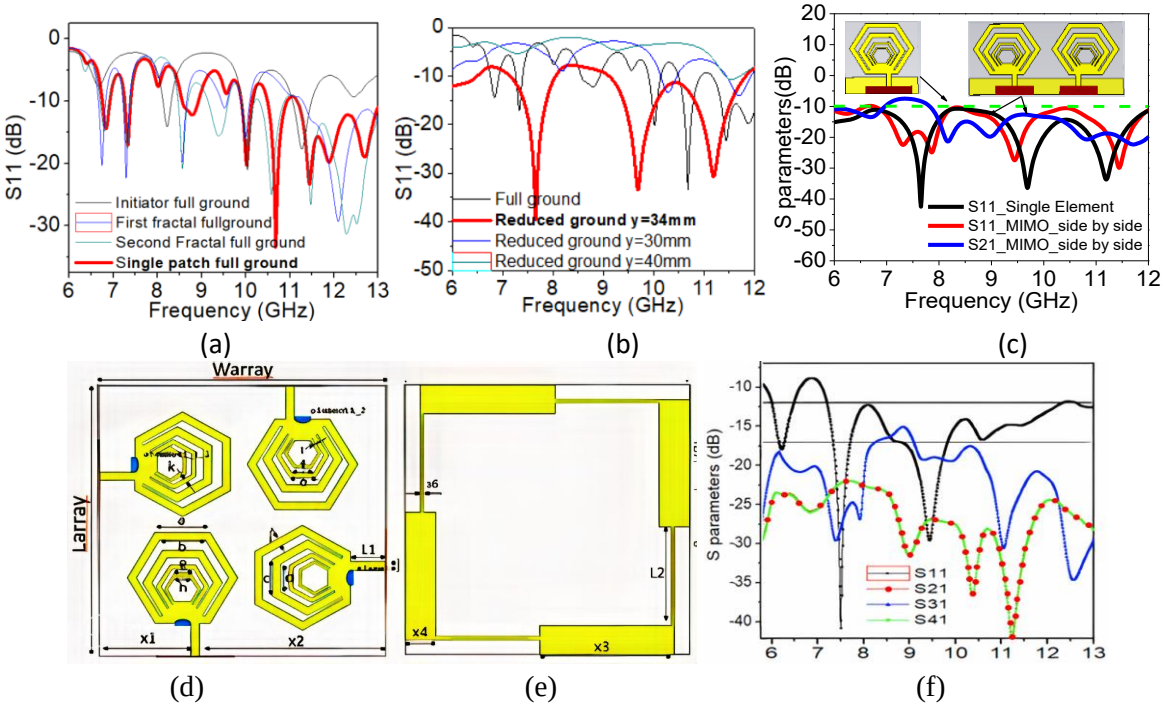

Figure 1. *(a) Evolution of Single Antenna (b) Effect of ground variation on S parameters (c) S parameter of single and two element MIMO (c) Front & back View of Four element orthogonally placed MPA (f) S parameters of Four element orthogonally placed MPA, (Reproduced courtesy of The Electromagnetics Academy) [24]*

The Adjustment width (w1) and length (l1, l7), helps in tuning the resonance frequency, The Inner Copper Patterns (w2, w3, l2, l3), create sub-resonances due to additional localized inductive-capacitive effects resulting in broadening the single negative frequency range. The Diagonal Copper Strips (w4), enhance current flow and suppress unwanted modes, improving the quality of the SNG behaviour. The central element, serves as a higher-frequency resonator within the unit cell and introduces new resonances at higher frequencies, expanding the frequency range for SNG properties. The gaps between conductive elements forms capacitive elements and helps in varying the resonant frequency. The unit cell works as a resonator by using its copper loops and gaps to create single-negative properties over a wide frequency range. The loops produce negative permeability through magnetic resonance, while the gaps cause negative permittivity through electric resonance. The design and dimensions of the copper are optimally adjusted to achieve SNG characteristics in UWB range.

The simulation setup prepared in CST 2018 used for extraction of effective parameters (permittivity and permeability) of metamaterial unit cell is shown in Figure 2 (b), in which the designed metamaterial is placed between wave ports in + z and -z direction along with perfect electric and magnetic boundaries in x and y directions respectively. The uniform plane wave is transmitted in z direction to mimic actual radiation as received through four element MIMO antenna. The Equations given below (1)-(3) are applied to extract permittivity and permeability of the proposed design in CST 2018 [15,28]. Figure 2(c) gives finally extracted characteristics of metamaterial which clearly shows the proposed design exhibit SNG (MNG + ENG) characteristics in C and X band

$$Z_{eff} = \pm\sqrt{\frac{(1+S11)^2-S21^2}{(1-S11)^2-S21^2}} \tag{1}$$

$$e^{jnk_o d} = \frac{S21}{1-S11\frac{z-1}{z+1}} \tag{2}$$

$$\varepsilon_{eff} = \frac{n_{eff}}{Z_{eff}} \quad , \quad \mu_{eff} = n_{eff} Z_{eff} \tag{3}$$

where Ko is the wave number, z_{eff} is impedance, d is thickness of the material, for present design its 1.6, ε_{eff}, μ_{eff} and n_{eff} are extracted effective permittivity, effective permeability, and effective refractive index of the material respectively. The metamaterial unit cell is fabricated in FR-4 substrate. (dielectric constant of 4.4 and a loss tangent (tan δ) of 0.025) with thickness of 1.6mm. The optimum dimensions of unit cell are given as (Figure 2 (d)) 14.6 x 14.6 x 1.6 mm3.The metamaterial unit cell is extended and optimized for 5 x 5 array structure to be placed above four elements orthogonal MPA as superstrate to improve diversity parameters.

2.3. Design of Four Element MIMO Loaded with Metamaterial Superstrate

To enhance the isolation between antenna elements, as discussed in the introduction section, designed 5 x 5 metamaterial structure is placed above MPA at 1.5mm height to achieve desired improvement in gain and isolation (Figure 2(e)). Spacers are used at the corners of the antenna to hold SNG metamaterial superstrate above the four element MIMO. Parametric optimization is done for height of superstrate above Microstrip patch antenna to determine the best position (H=1.5mm) which also confirms the compact 3d design of the present work along with best improvement in isolation and gain. The spacing between meta surface and MIMO is very important parameter to achieve high gain while allowing only the constructive interference between the antenna generated wave and meta surface reflected wave. The proposed design achieves isolation enhanced to more than -28 dB throughout C and X band as shown in Figure 2 (f). The metamaterial superstrate improves in isolation parameters (S21=-22dB, S31=-13dB and S41=-22dB) in without metamaterial case to minimum -28 dB in the entire impedance bandwidth in case of of four element orthogonally placed MIMO with metamaterial superstrate. The scattered Gain vs frequency plot with amount of gain improvement achieved at certain frequency is shown in Figure 2 (g) which shows that design with metamaterial offers improvement in gain constantly with maximum gain improvement of 1.62dBi. Final Gain vs frequency plot with metamaterial is shown in Figure 2(h), which clearly shows that the proposed antenna offers appreciable gain (more than 3dBi) in the entire UWB range of 6-12GHz with peak gain 5.8dBi.

3. EXPERIMENTAL VERIFICATION & RESULT ANALYSIS

Orthogonally placed Four element MIMO loaded with Metamaterial superstrate is fabricated and tested with two port Agilent N5247 vector network analyzer (VNA) for S parameters and VSWR measurement. During measurement, designed UWB antenna is used as receiving antenna, only one port is connected to VNA and the other port is terminated with 50-ohm matched load. Radiation pattern measurement was conducted inside microwave anechoic chamber to avoid losses in the measurement as shown in Figure 3 (a), (b) and (c). Designed metamaterial is placed above four element MIMO at 1.5mm height as shown in Figure 3(d). Slight deviation in simulated and measurement results were observed in S parameters results but still they verified the simulation results perfectly.

3.1. Result & Discussion

The measured reflection coefficient and VSWR shown in Figure 3 (e) shows that the proposed antenna gives resonance bandwidth in C and X band with good impedance matching. The application of metamaterial superstrate results in improved S parameters (specially S21, S31 and S41) as compared to four element orthogonally placed MIMO without metamaterial shown in Figure 1(f). The measured S parameters obtained are in close agreement with simulation results as shown in Figure 3(f) and 3(g). The measured isolation parameters are well below -30 dB in the full resonance band.

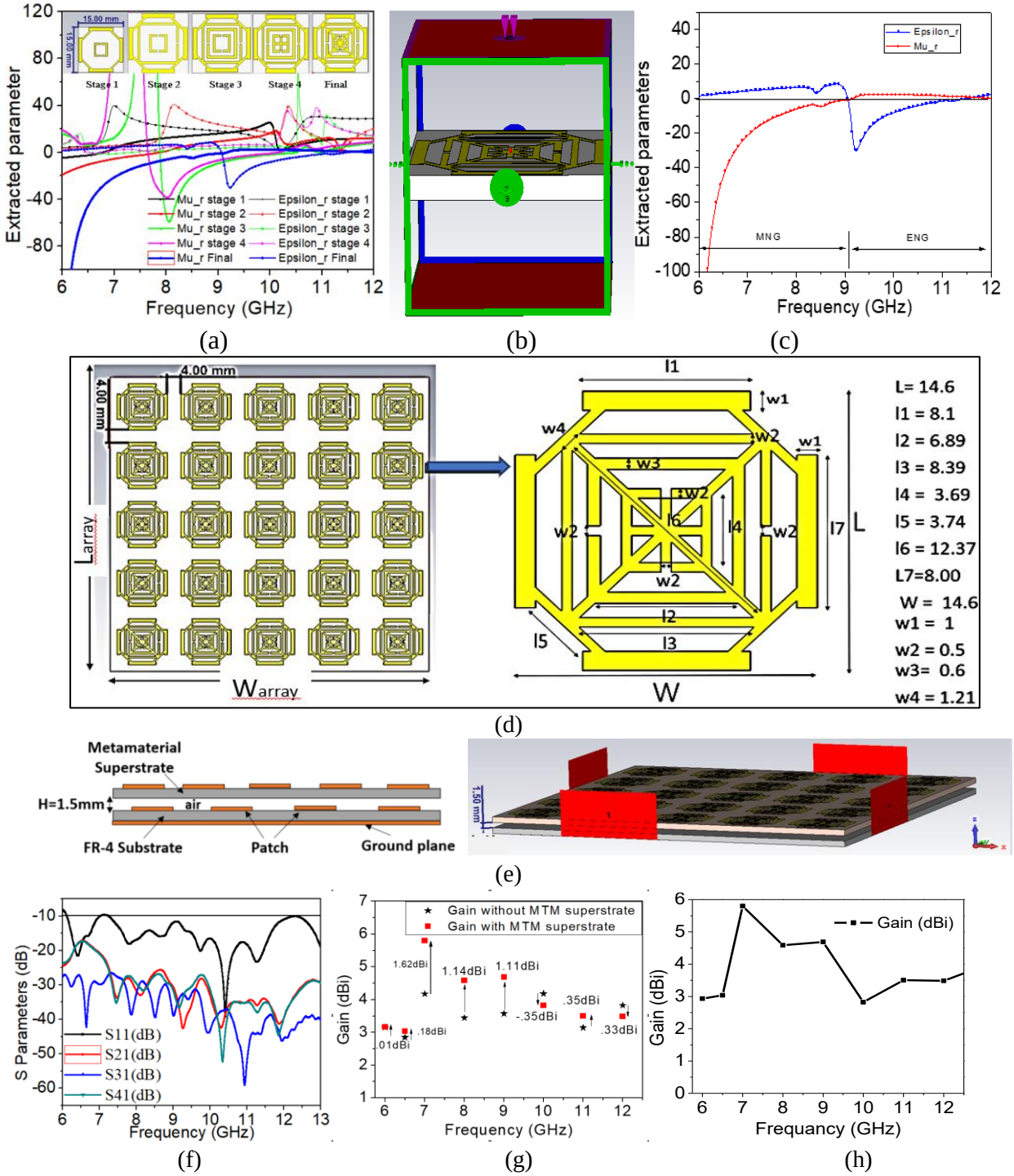

Figure 2. *(a) Evolution of metamaterial with extracted material parameter (b) Simulation Setup (CST) for Extraction of parameter (c) Extracted parameters of Final metamaterial (d) 5 x 5 array of metamaterial unit cell with design dimension of unit cell (e) metamaterial superstrate loaded MPA (f) S parameters with metamaterial (g) Gain Vs frequency without and with metamaterial structure (h) Gain of final design*

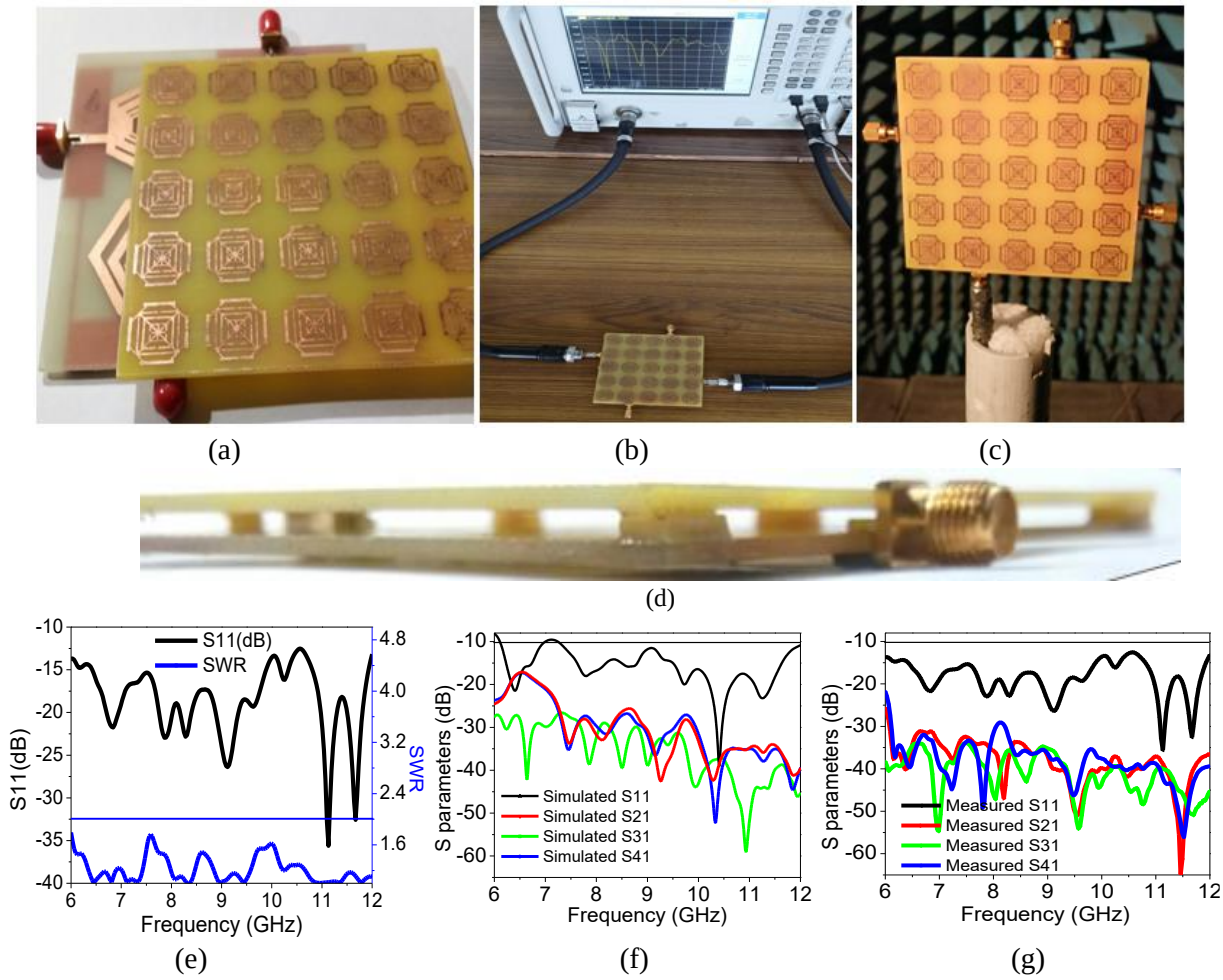

Figure 3. *(a) Fabricated Four element MPA loaded with metamaterial (b) VNA Testing (c) Field pattern testing (d) placement of metamaterial above antenna using spacer (e) Measured S parameters and VSWR (f) Simulated S parameters (g) Measured S parameters*

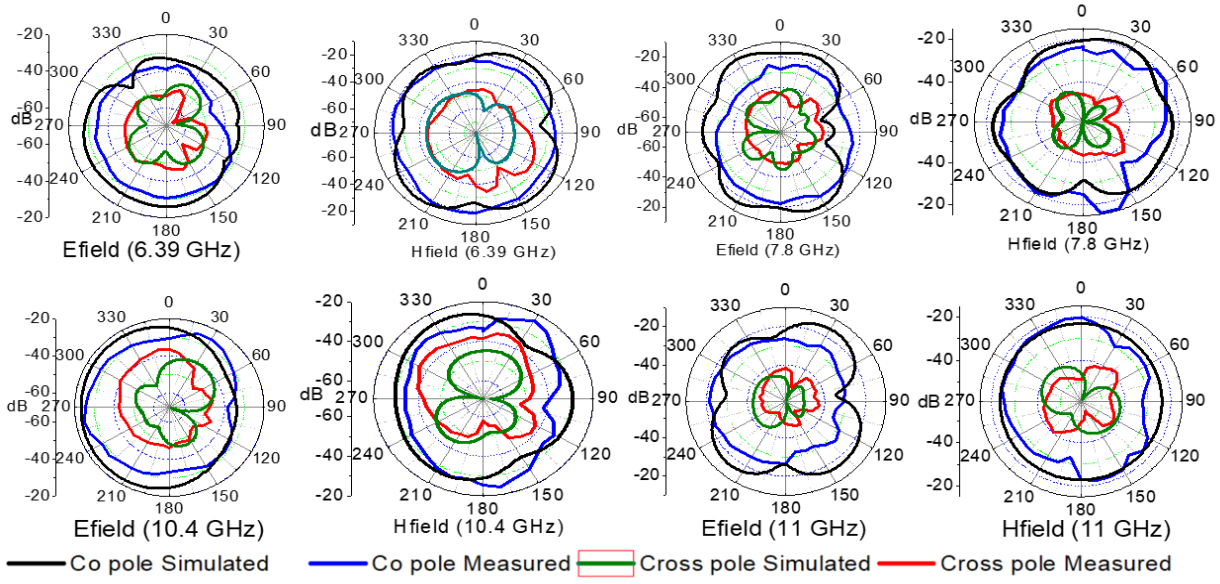

Figure 4. *Measured 2D Radiation pattern for E field and H field*

The Measured E field and H filed radiation pattern are drawn in Figure 4, which shows more co-polarization and less cross polarization with almost omnidirectional radiation pattern at 6.39GHz, 7.8GHz, 10.4GHz, 11GHz. The proposed antenna is also tested for diversity parameters like Envelope correlation coefficient (ECC), Diversity Gain (DG), Channel capacity loss (CCL), and mean effective gain (MEG) by calculating them using the Equation (4)-(8) given below [24]

$$\text{ECC } \rho_{12} = \frac{|S_{11}^{*}S_{12}+S_{21}^{*}S_{22}|^2}{(1-|S_{11}|^2-|S_{21}|^2)(1-|S_{22}|^2-|S_{12}|^2)} \tag{4}$$

$$\text{DiversityGain} = \left[\frac{\gamma_c}{\text{SNR}_c} - \frac{\gamma_1}{\text{SNR}_1}\right]_{P(\gamma_c<\gamma_s/\text{SNR})} \tag{5}$$

$$\text{Channel capacity loss } C_{loss} = -\log_2|\psi^R| \tag{6}$$

$$\psi^R = \begin{bmatrix} \varrho_{11} & \varrho_{12} \\ \varrho_{21} & \varrho_{22} \end{bmatrix} \tag{7}$$

where ψ^R is the receiving antenna correlation matrix

and $\varrho_{ii} = (1-|S_{ii}|^2 - |S_{ij}|^2)$ and $\varrho_{ij} = (S_{ii}^{*}S_{ij} + S_{ji}^{*}S_{ij})$ for i, j=1 or 2

$$\text{MEG}_i = 0.5\ (1 - \sum_{j=1}^{k}|S_{ij}|^2) \tag{8}$$

where k represents number of antennas, i is the antenna under consideration for calculating Mean effective gain.

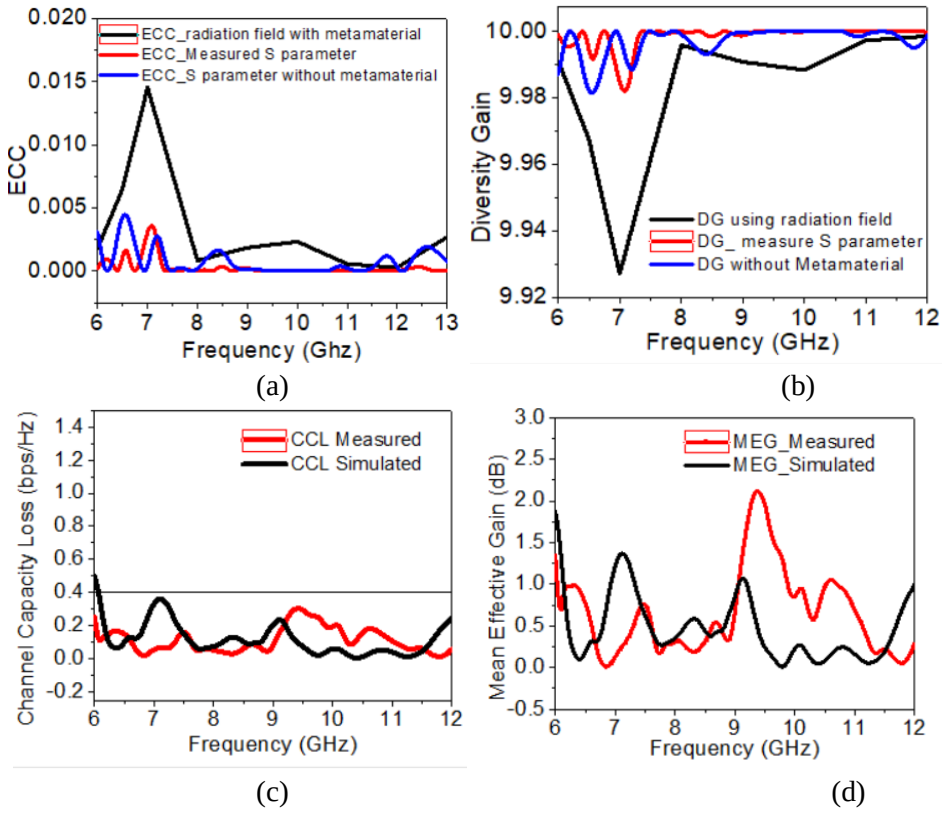

Figure 5. *(a) ECC using both radiation field and S parameters (b) DG (c) CCL Measured and simulated (d) MEG (measured and simulated) for the proposed design*

ECC and DG calculated using Equation (4) and (5) are well below the acceptable range from both S parameters and radiation field, the obtained results are <0.015 (radiation field), <.005 (S parameters) and >9.92 (radiation field), >9.98 (s parameters) respectively as shown in Figure 5 (a) and 5 (b) respectively. The Figure 5 (a) and 5 (b) gives comparison of ECC and DG without metamaterial and with metamaterial

(Measured as well as radiation filed). CCL is calculated using Equation (6)-(7) for both simulation and measurement data and are obtained to be < 0.4 bps/Hz (acceptable range) throughout the band as shown in Figure 5(c). MEG is calculated using Equation (8) for both simulated and measured results and are obtained below 3dB (acceptable range) throughout C and X band (Figure 5(d)). Table 1 shows the comparison of the proposed design with already published literature with respect to parameters like volume, size, bandwidth, measured gain, ECC, DG, isolation, and complexity of the design. The comparison shows that the proposed design gives minimum volume with superstrate structure, covers more bandwidth with low-cost FR-4 material with less complex design. The uniqueness of the proposed design is its less volume despite the metamaterial superstrate placed 1.5 mm above the MIMO. The compact volume and good diversity parameters result this design to be effective for wireless applications.

Table 1. *Comparison of proposed work with already published literatures*

Ref	No. of element & Substrate	EtEd (mm)	Size (mm)	Operating Band (GHz)	Peak Measured Gain (dBi)	Isolation (dB)	design complexity	Application Covered
[13]	4 (FR-4)	NA	52 x 52 x 1.6 h= 27.2 height	3.6–18	4	Better than 15	High design volume due height of metamaterial	Super wideband antenna
[18]	4 (Rogers)	22	80 x 80 x 1.575 With **h=12**	3.11 - 7.67	8.3	Better than 15.5	High design volume due to metamateial height	5G Sub6 GHz MIMO systems
[19]	4 (FR-4)	12.5	60 × 60 x 1.6 **h=12.5**	(3.25–5.6)	7.1	Better than 35	High design volume due to height of metamaterial	MIMO applications in the 5G NR n77/n78/n79 spectrums.
[20]	4 (Rogers)	57.9	146 × 146 × **3.118**	3.27 - 3.82	8.72	Better than 32	Slots and isolating pin	5G Sub6 GHz (n78 band) MIMO systems
[21]	2 (FR-4)	18.4	83.8 × 83.8 × 3.2 **h=15**	2.23–2.91	7.02	Better than 14.5	High design volume due to height of metamaterial	satellite applications
[22]	2 (FR-4)	20	70 x 37 x 1.6	(8.7-11.7), (11.9-14.6), (15.6-17.1) (22-26), (29-34.2)	9.15 (at 26 GHz) 6 in X band	Better than 20	Hilburt Fractal design loaded is difficult for higher order	MIMO and radar systems
[23]	4 (Rogers)	3	70 x 60 x 0.8 h= **9**	5.65 - 6.06	8.5	Better than 28	High design volume due height of metamaterial	WLAN only
[24]	4 (FR-4)	5.5	93 x 93 x 1.6	3-13 GHz	5.4 dBi	Better than 15	Loading of resistance.	C and X band Applications
[25]	4 (Rogers)	12	178 x 178 x 14	2.76–4.3 GHz	6.2 to 10.5 (3-4 GHz)	Better than 23	Metamaterial with periodic loading	5G Antenna
[26]	4 (Rogers)	57.9	146 x 146 1.5 h= 3.048	3.3-3.87 GHz	8.72	Better than 32	High design volume due double substrate	5G sub 6 GHz
This Work	**4 (FR-4)**	**5.5**	**93 x 93 x 4.7 h=1.5**	**6-12 band**	**5.79**	**Better than 30**	**Simple to design and optimize**	**C-band/ Entire X Band applications**

4. CONCLUSION

In this paper, An SNG metamaterial superstrate is proposed for effective reduction in mutual coupling in four element orthogonally placed MIMO antenna. The MIMO is fabricated and the experimental results shows isolation more than -30dB in the entire resonance band from C to X band with gain of more than 3dBi in the entire range (peak gain of 5.8dBi). The omnidirectional E field and H field patten shows desired less cross polarization. The uniqueness of the proposed design is that, the metamaterial superstrate placed at a very short distance of 1.5 mm results much less volume with already published works as given in comparison Table 1. The proposed design can decouple closely packed four element MIMO antennas with edge-to-edge separation of 0.33λg. The design with compact volume and good diversity parameters gives

a unique idea of placement of metamaterial superstrate at a very short distance of 1.5 mm that covers entire C and X band applications.

CONFLICTS OF INTEREST

No conflict of interest was declared by the authors.

ETHICAL APPROVAL

This work has been carried out ethically, keeping in mind privacy, consent, and appropriateness of related data.

ACKNOWLEDGEMENTS

The authors Acknowledge *The Electromagnetics Academy* for giving permissions to reproduce figures. The authors declare that no agency or organization have funded the work performed in direct or indirect way to get acknowledge.

REFERENCES

[1] Sharawi, M. S., "Printed multi-band MIMO antenna systems and their performance metrics [Wireless Corner]", IEEE Antennas and Propagation Magazine, 55(5): 218–232, (2013). DOI: 10.1109/MAP.2013.6685359.

[2] Mark, R., Mishra, N., Mandal, K., Sarkar, P.P., Das, S., "Hexagonal ring fractal antenna with dumbbell shaped defected ground structure for multiband wireless applications," AEU - International Journal of Electronics and Communications, 94: 42–50, (2018). DOI: 10.1016/j.aeue.2018.06.015.

[3] Arora, C., Pattnaik, S. S., and Baral, R. N., "Dual band microstrip patch antenna array loaded with split ring resonators and via holes", AEU - International Journal of Electronics and Communications, 93: 253–260, (2018). DOI: 10.1016/j.aeue.2018.07.013.

[4] Gupta, S. K., Sharma, A., and Das, S., "Gain and isolation enhancement of MIMO antenna for WLAN applications", IEEE Microwaves, Antennas, and Propagation Conference (MAPCON), Bangalore, India, 692-697, (2022). DOI: 10.1109/MAPCON53227.2022.9741421.

[5] Abdelhamid, C., Sakli, H., and Sakli, N., "A four-element UWB MIMO antenna using SRRs for application in satellite communications", International Journal of Electrical and Computer Engineering, 11(4): 3154–3167, (2021). DOI: 10.11591/ijece.v11i4.

[6] Wu, W., Yuan, B., and Wu, A., "A quad-element UWB-MIMO antenna with band-notch and reduced mutual coupling reduction based on EBG structures", International Journal of Antennas and Propagation, 2018, ID 8490740, (2018). DOI: 10.1155/2018/8490740.

[7] Malaisamy, K., Santhi, M., and Robinson, S., "Design and analysis of 4 × 4 MIMO antenna with DGS for WLAN applications", International Journal of Microwave and Wireless Technologies, 13(9): 979–985, (2021). DOI: 10.1017/S1759078721000495.

[8] Bhanumathi, V., and Sivaranjani, G., "High isolation MIMO antenna using semi-circle patch for UWB applications", Progress in Electromagnetics Research C, 92: 31-40, (2019). DOI: 10.2528/PIERC19051304.

[9] Pannu, P., and Sharma, K. D., "Miniaturize four-port UWB-MIMO antenna with tri-notched band characteristics," Microwave and Optical Technology Letters, 63(5): 1489–1498, (2021). DOI: 10.1002/mop.32766.

[10] Gao, D., Cao, Z., Quan, X., Xu, C., Chen, P., "A complementary split-ring array for compact decoupling 2 × 2 circularly polarized antenna", Microwave and Optical Technology Letters, 63(4): 1294–1303, (2021). DOI: 10.1002/mop.32828.

[11] Wang, F., Duan, Z., Li, S., Wang, Z.L., Gong, Y.B., "Compact UWB MIMO Antenna with Metamaterial-inspired Isolator", Progress in Electromagnetics Research C, 84: 61-74, (2018). DOI: 10.2528/PIERC18041602.

[12] Zhu, X., Yang, X., Song, Q., Lui, B., "Compact UWB-MIMO antenna with metamaterial FSS decoupling structure", EURASIP Journal on Wireless Communications and Networking, 1, (2017). DOI: 10.1186/s13638-016-0783-2.

[13] Aggarwal, I., Pandey, S., Tripathy, R. M., Mittal, A., "A super wideband MIMO antenna with metamaterial superstrate for gain enhancement at WLAN frequency band", International Journal of Systems Assurance Engineering and Management, 14(2): 643–658, (2023). DOI: 10.1007/s13198-022-01675-5.

[14] Faruque, I. R. M., Siddiky, M. A., Ahamed, E., Islam, M. T., Abdullah, S., "Parallel LC shaped metamaterial resonator for C and X band satellite applications with wider bandwidth", Scientific Reports, 11(1): (2021). DOI: 10.1038/s41598-021-97066-3.

[15] Rajak, N., Chattoraj, N., and Mark, R., "Metamaterial cell inspired high gain multiband antenna for wireless applications", AEU - International Journal of Electronics and Communications, 109: 23–30, (2019). DOI: 10.1016/j.aeue.2019.07.001.

[16] Gao, X., Zhang, Y., and Li, S., "High refractive index metamaterial superstrate for microstrip patch antenna performance improvement", Frontiers in Physics, 8, (2020). DOI: 10.3389/fphy.2020.557070.

[17] Asadpor, L., Sharifi, G., and Rezvani, M., "Design of a high-gain wideband antenna using double-layer metasurface", Microwave and Optical Technology Letters, 61(4): 1004–1010, (2019). DOI: 10.1002/mop.31767.

[18] Jabire, H. A., Ghaffar, A., Li, X.J., Abdu, A., Saminu, S., "Metamaterial based design of compact UWB/MIMO monopole antenna with characteristic mode analysis", Applied Sciences, 11(4): 1–21, (2021). DOI: 10.3390/app11042121.

[19] Hasan, M. M., Islam, M. T., Rahim, S. K. A., Alam, T., Rmili, H., Islam, Md. S., Soliman, M. S., "A compact mu-near-zero metamaterial integrated wideband high-gain MIMO antenna for 5G new radio applications", Materials, 16(4): 1751, (2023). DOI: 10.3390/ma16041751.

[20] Sufian, A. M., Hussain, N., Askari, H., Park, S.G., Shin, K. S., Kim, N., "Isolation enhancement of a metasurface-based MIMO antenna using slots and shorting pins", IEEE Access, 9: 73533-73543, (2021). DOI: 10.1109/ACCESS.2021.3077243.

[21] Ameen, M., Ahmad, O., and Chaudhary, R. K., "Wideband circularly-polarised high-gain diversity antenna loaded with metasurface reflector for small satellite applications", Electronics Letters, 55: 829-831, (2019). DOI: 10.1049/el.2019.1645.

[22] Alibakhshikenari, M., Khalily, M., Virdee, S. B., See, C. H., Abd-Alhameed, R. A., Limiti, E., "Mutual coupling suppression between two closely placed microstrip patches using EM-bandgap metamaterial fractal loading", IEEE Access, 7: 23606-23614, (2019). DOI: 10.1109/ACCESS.2019.2891861.

[23] Mark, R., Rajak, N., Mandal, K., and Das, S., "Isolation and gain enhancement using metamaterial-based superstrate for MIMO applications", Radioengineering, 28: 689-695, (2019). DOI: 10.13164/re.2019.0689.

[24] Gupta, S. K., Mark, R., Mandal, K., and Das, S., "Four element UWB MIMO antenna with improved isolation using resistance loaded stub for S, C and X band applications", Progress in Electromagnetics Research C, 131, 73-87, (2023).

[25] Salehi, M., Oraizi, H., "Wideband high gain metasurface-based 4T4R MIMO antenna with highly isolated ports for sub-6 GHz 5G applications", Scientific Reports, 14, 14448, (2024). DOI: 10.1038/s41598-024-65135-9.

[26] Sufian A. M., Hussain N., Askari H., Park G. S., Shin S. K. and Kim N., "Isolation Enhancement of a Metasurface-Based MIMO Antenna Using Slots and Shorting Pins", IEEE Access, 9: 73533-73543, (2021). DOI: 10.1109/ACCESS.2021.3079965.

[27] Rahman Md. A, Al-Bawri S. S., Abdulkaw M. W., Aljaloud K., Islam T. M., "A unique SWB multi-slotted four-port highly isolated MIMO antenna loaded with metasurface for IOT applications-based machine learning verification", Engineering Science and Technology, an International Journal, 50: 101616, ISSN 2215-0986, (2024). DOI: 10.1016/j.jestch.2024.101616.

[28] Smith, D., Vier, D., Koschny, T., and Soukoulis, C. M., "Electromagnetic parameter retrieval from inhomogeneous metamaterials", Physical Review E, 71(3): 036617, (2005). DOI: 10.1103/PhysRevE.71.036617